2021 10th International IEEE/EMBS Conference on Neural Engineering (NER)
Virtual Conference, May 4-6, 2021

Correlated inputs to striatal population drive subthalamic nucleus hyper-synchronization

Elena Manferlotti, Matteo Vissani, Alberto Mazzoni^, Arvind Kumar^

Abstract— **Movement disorders such as Parkinson's disease (PD) are often associated with hyper-synchronization in basal ganglia (BG) activity. The origins of the hyper-synchronization and its interaction with deep brain stimulations (DBS) of BG nuclei are still debated. The structure of the BG suggests that strong neuronal correlations cannot arise within the BG but should rather be inherited from cortical or thalamic inputs. However, this is inconsistent with the hypothesized de-correlating role of the striatal network. Here we investigate to what extent striatum can decorrelate correlated inputs, and the consequences of correlations in striatal activity on the dynamics of the BG; especially, the beta-band oscillations, which are the cardinal symptom of PD. We developed a BG network model with spiking neurons and analyzed the effects on input correlation on BG activity. We found that striatum does not completely decorrelate the inputs and that the residual correlations can synchronize the whole BG. These results provide new insights into the origin of BG hyper-synchronization and pave the way to understand DBS induced disruption of synchrony and ensuing therapeutical effects.**

I. Introduction

Neural recordings acquired with DBS electrodes BG have contributed immensely to the understanding of BG physiopathology in movement disorders [1], [2]. Behavioral deficits of patients with PD are accompanied by increased bursting activity [3] and synchrony in most of BG nuclei [4]–[6]. Moreover, at the population level, PD patients present an aberrant oscillation in the beta band (13-30 Hz), which correlates with some cardinal motor symptoms of the disease, e.g., rigidity and bradykinesia [7]. Both computational models [8], [9] and experimental data [4], [10] suggest that increased firing rate of D2 type striatal projection neurons (SPN) could cause both oscillations and hyper-synchrony in the BG. Bursts of beta band oscillations are also associated with increased synchrony in the striatum [11]. Given the sparse and weak connectivity within the striatum it is unlikely that experimentally observed synchrony can arise locally within the striatum. In fact, striatum is thought to be a decorrelating network [12]. This suggests that PD related changes break the decorrelation mechanism of the striatum. Alternatively, it is also possible that the striatum is driven by more correlated input from the cortex and the thalamus. Surprisingly, the extent to which striatum can decorrelate inputs has not been quantified, neither experimentally nor in computational models, and it is not clear whether striatal correlation can induce oscillations and synchrony in the downstream nuclei. Understanding of the origin and modulation of synchrony and oscillations is necessary to fully determine how pathological oscillatory activity impairs motor processing in PD.

Here, we investigated the decorrelating function of the striatum and effect of correlations within the striatal activity on the activity of downstream nuclei of the BG. We injected cortical-correlated inputs into the striatum and measured synchrony and oscillations in the BG network. Correlations in the striatum induced synchrony and oscillations in beta frequency range, without changing firing rates of those striatal populations. These results provide new insights into the origin of pathological neuronal activity associated with PD.

II. Methods

We adopted an already established computational model of the BG [13] to characterize how correlated inputs to the striatum reverberate throughout the network's dynamics. The model structure is depicted in Fig. 1A. The network consisted of 15128 neurons distributed in seven neuronal populations: D1 and D2 type dopamine receptor expressing SPNs (D1 and D2 SPNs), fast spiking interneurons (FSNs), subthalamic nucleus (STN), globus pallidus internal (GPi). Neurons in the globus pallidus external (GPe) have been split into arkypallidal (GPTA) and prototypical (GPTI) [14]. The number of neurons in each subnuclei was chosen according the relative size of BG subnuclei [13], [15]. The in-degree of each neuron was fixed and within and between BG subnuclei connections were formed randomly with fixed a connection probability (See Table 1).

A. Model inputs: background activity and correlated inputs

All neurons in the network received external uncorrelated Poisson type spike trains with a fixed rate ($Input_{rate}$) selected to induce firing rates close to *in vivo* measurements (D1- and D2-SPNs: 2-5Hz [16], FSNs: 10-20Hz, GPTA: 5-10Hz, GPTI: 30-50Hz, STN: 20Hz [17], GPi: ~30Hz). The input was later divided into a correlated and uncorrelated component. The correlated inputs were generated using the following steps for each striatal population: (i) we created *N* (= size of the population) copies of a Poisson type spike train

E. Manferlotti, is with The BioRobotics Institute and Department of Excellence in Robotics and AI, Scuola Superiore Sant'Anna, Pisa, 50127 Italy (e-mail: elena.manferlotti@santannapisa.it).

M. Vissani is with The BioRobotics Institute and Department of Excellence in Robotics and AI, Scuola Superiore Sant'Anna, Pisa, 50127 Italy (e-mail: matteo.vissani@santannapisa.it).

A. Mazzoni is with The BioRobotics Institute and Department of Excellence in Robotics and AI, Scuola Superiore Sant'Anna, Pisa, 50127 Italy (e-mail: alberto.mazzoni@santannapisa.it).

A. Kumar is with the Division of Computational Science and Technology, KTH Royal Institute of Technology, Stockholm, 100 44 Sweden. (email: arvkumar@kth.se).

A. Mazzoni and A. Kumar share same senior author contribution.

2021 10th International IEEE/EMBS Conference on Neural Engineering (NER) | 978-1-7281-4337-8/21/$31.00 ©2021 IEEE | DOI: 10.1109/NER49283.2021.9441370

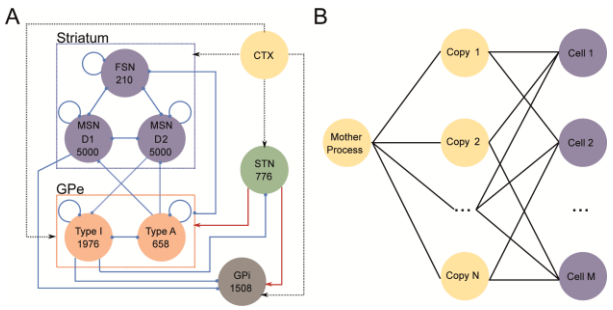

Figure 1. **Basal ganglia network and input architectures**. A: Schematic illustration of the populations included in the basal ganglia model specifying the number of neurons in each simulated nucleus. Inhibitory (solid blue lines with round arrowheads) and excitatory (solid red triangular arrowheads lines) synapses are displayed. The cortical input is depicted with dotted black lines with triangular arrowheads. B: Architecture of the correlated input. The Poissonian mother process is copied in an intermediate layer of neurons having the same number of cells of the target populations (D1, D2, FSNs). It ensures the reproducibility of the starting input signal. Each cell in the last layer receives the same number of incoming projections. This is a function of the desired correlation coefficient that we want to inject and the number of neurons in the target population.

(mother" process M), and (ii) we injected C_{in} spike trains to each neuron in the target population.

The number C_{in}depends on the desired input correlation (ρ_{cs}) and N (Figure 1B) such that C_{in}(D1 − and D2 − SPNs) = [100, 500] and C_{in}(FSNs) = [4, 21]. The rate of the mother process M (Eff_{rate}) was computed as a function of the input rate and the number of connections C_{in} necessary to achieve a certain amount of pairwise correlation:

$$Eff_{rate} = \frac{Input_{rate}}{C_{in}} = \frac{Input_{rate}}{\rho_{cs} N} \qquad (1)$$

Input correlation ρ_{cs} was then varied in the range [0, 0.1] without varying the input firing rate using the same synaptic weights of the uncorrelated Poisson noise.

B. Neuron and synapse model

All neurons were modeled as point neurons described using two versions of the conductance-based leaky integrate-and-fire model, which allows to adequately study the BG dynamics. The evolution of the membrane potential $V(t)$ in D1-, D2-SPN, and FSNs was described by (2):

$$C_m \frac{dV(t)}{dt} = -g_L(V(t) - E_L) - \sum_j g_j(t)\big(V(t) - E_j\big) + I \qquad (2)$$

TABLE I. *NUMBER OF SYNAPTIC CONNECTIONS AMONG POPULATIONS.*

Population		Presynaptic population						
		SPN_{D1}	SPN_{D2}	FSN	GPe_{TA}	GPe_{TI}	STN	GPi
Postsynaptic target	SPN_{D1}	728	784	32	20	-	-	-
	SPN_{D2}	784	1008	22	20	-	-	-
	FSN	32	22	20	20	20	-	-
	GPe_{TA}	-	-	20	10	50	60	-
	GPe_{TI}	-	1000	20	10	50	60	-
	STN	-	-	-	-	60	-	-
	GPi	1000	-	-	-	64	60	-

where C_m denotes the membrane capacitance, g_L is the leakage conductance, E_L and E_j are the reverse potentials, and I is the external input. The post-synaptic conductance $g_j(t)$ of the striatal neurons were modelled by an α-function (3):

$$g_j(t) = \frac{t - t_{spk}}{\tau_{syn_j}} \exp\left(1 - \frac{t - t_{spk}}{\tau_{syn_j}}\right) \qquad (3)$$

Here, τ_{syn_j} is the synaptic time constant. STN, GPTA, GPTI and GPi neurons were described by an adaptive exponential integrate-and-fire according to the following:

$$C_m \frac{dV(t)}{dt} = -g_L(V(t) - E_L) - \sum_j g_j(t)\big(V(t) - E_j\big) + g_L \Delta_T \exp\left(\frac{V(t) - V_{th}}{\Delta_T}\right) - \sum_j g_j(t)\big(V(t) - E_j\big) - w(t) + I_e \qquad (4)$$

$$\tau_m \frac{dw(t)}{dt} = a(V(t) - E_L) - w(t) \qquad (5)$$

where w(t) is the adaptation current. The post-synaptic conductance $g_j(t)$ were modelled as follows [18]:

$$g_j(t) = \frac{t - t_{spk}}{\tau_{syn_j}} \exp\left(-\frac{t - t_{spk}}{\tau_{syn_j}}\right) \qquad (6)$$

C. Data analysis

We discarded the first 100 milliseconds of initial network transients. The population synchrony index (Fano Factor FF_{pop}) of the population spike count is the ratio of the population spike count variance (σ^2_{pop}) and the mean number of spikes (m_{pop}). An ensemble of independent Poisson processes yields FF_{pop} = 1, whereas positive correlations in the population activity result in $FF_{pop} > 1$.

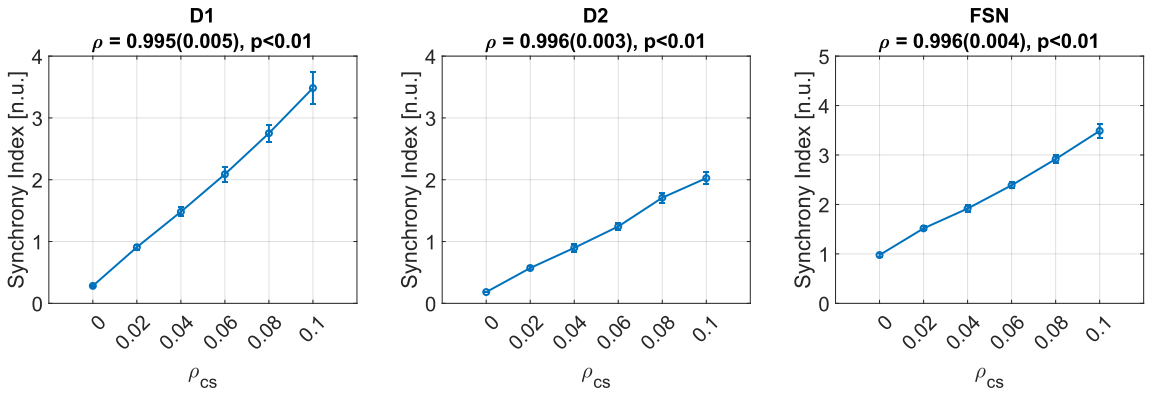

Figure 2. **Effects of input correlation on target populations.** Synchronicity index as a function of input correlation for the three striatal populations. Points and error bars represent the values of mean and standard deviation of the distribution, respectively. Title reports the mean and the standard deviation of the correlation between the two variables and its significance.

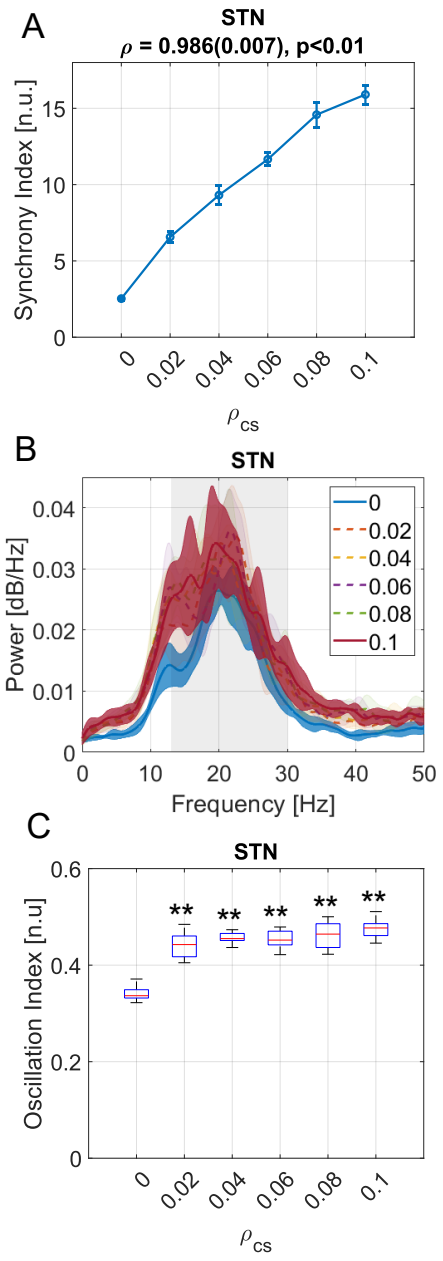

Figure 3. **Striatal synchronicity reverberates in downstream nuclei**. Mean synchronicity index trend as a function of input correlation for the two populations. Error bars show the standard deviation of each distribution. Title reports correlation between the two values and its significance in the format mean(std). C: Oscillatory index of the two populations as a function of input correlation. Markers (**) indicate p < 0.01 significant difference from the baseline.

Finally, we computed the power spectrum $P(f)$ of the binned (bin width = 2 ms) and z-scored population activity using the periodogram method (Fs = 500Hz, points = 2048). The presence of beta oscillations (13-30 Hz) we defined the following oscillation index OI_{pop}:

$$OI_{pop} = \frac{\int_{13}^{30} P(f)df}{\int_{0}^{Fs/2} P(f)df} \quad (7)$$

In case of strong oscillations OI_{pop} is close to unity.

D. Implementation

All simulations were implemented using the simulation environment NEST (ver. 2.16.0) [19] with a discretization step of $\Delta T = 0.1$ms. Simulation lasted 5 seconds.

III. Results

We investigated the perturbation in BG dynamical activity driven by the injection of synchronized cortical input to the striatum. We varied the input correlation ρ_{cs} among cortical spiking trains from 0 to 0.1.

A. Local effects of input correlation on target nuclei

We investigated how input correlation affected dynamics in recipient areas. We observed that a correlated input led to a significant (ANOVA, $p < 0.01$) increase in D1-SPN and FSNs firing rates (+6.57% +16.52%). Post-hoc analysis revealed that firing rate was significantly ($p<0.01$, post-hoc ANOVA) higher than the baseline for correlation above 0.06 in D1-SPN and 0.04 in FSNs. D2-SPN firing rate was not affected by input correlation (ANOVA, $p = 0.64$(0.45) mean(std)). In the striatum, population synchrony monotonically increased as a function of input correlations (ANOVA, $p < 0.01$) (D1-SPN [2.83 – 34.83], D2-SPN [1.82 – 20.25], FSN [0.98 – 3.49], Fig. 2). Input correlations are then not completely decorrelated by striatal network.

B. Downstream effects of input correlation

We then questioned to what extent synchrony in the striatum is propagated to the downstream nuclei. The GPe neurons receive inhibitory projections from the striatum and are connected to the STN, through an excitatory-inhibitory synaptic projection. The local connectivity within the GPe and its interactions with the STN can modulate the input synchrony. In our model, striatal correlation was transferred to the GPe and STN activity, i.e., the network downstream to the striatum failed to decorrelate input dynamics (Fig. 3A). Temporal correlations within the STN population [2.53 – 15.90] were proportional to input correlation (Fig. 3A).

The enhanced synchrony in the striatum also led to a change in the oscillations in the GPTI-STN loop. Spectral analysis of STN activity revealed the presence of a well-defined peak in the beta band (Fig. 3B). This peak emerged as the temporal correlation in striatal input were increased. Post-hoc analysis shows a significant (post-hoc ANOVA, $p<0.01$) increase beta band power as the network becomes more synchronized. The OI (Methods) shows how STN fluctuations become significantly more sustained with respect to the background activity (post-hoc ANOVA $p<0.01$, between baseline and all other values, Fig. 3c). However, unlike synchrony, the OI quickly saturated for striatal correlation at as low a value as 0.04. This suggests that a small increase in the input correlation can enhance oscillations but oscillations strength may not correlate with the amount of input correlations or degree of synchrony in the striatum.

IV. Discussion

We found that the local connectivity of the striatum – at least the elements included in our model – is not sufficient to decorrelate even small input correlations. Striatal

synchronicity reverberates in the whole network leading to a monotonic increase of the firing rate and synchrony in STN as the injected correlation becomes stronger.

We found that very low levels of input correlation are sufficient to induce significant increase in synchrony, and, in particular, an increase in beta power in the STN. However, the synchronized beta activity also saturated quickly for relatively low levels of input correlation. This suggests a threshold like sensitivity of the beta resonance to input correlation. Periodic pairwise correlated bursting activity have been frequently reported in *in vivo* recorded neuronal spike trains from several brain regions [20], [21]. In the BG, correlation can also have functional and dysfunctional consequences by eliciting beta-band oscillations. While low-power and short-duration beta oscillations bursts are necessary for action inhibition [22], high-power and long-lasting beta bursts can completely block actions (as is seen in PD [23]). Much has been discussed about the origin of beta oscillations [3] [24]. Now we provide evidence that correlations in the striatum can also induce beta oscillations.

We expect that at higher input firing rates, input correlations may have even stronger effect on beta oscillations. In addition, the altered imbalance of D1- and D2-SPNs firing rates in PD can further enhance synchrony in the striatum and its downstream impact on oscillations.

V. Conclusion

Our results show that correlations in the striatal activity can cause increase the oscillations and synchrony in the BG – both are pathologically enhanced in the PD. These results suggest that therapeutic measures such as DBS may also reduce pathological activity by decorrelating the BG spiking activity.

References

[1] P. Brown, «Abnormal oscillatory synchronisation in the motor system leads to impaired movement», *Current Opinion in Neurobiology*, vol. 17, n. 6. Elsevier Current Trends, pagg. 656–664, dic. 01, 2007, doi: 10.1016/j.conb.2007.12.001.

[2] M. Vissani, I. U. Isaias, e A. Mazzoni, «Deep brain stimulation: a review of the open neural engineering challenges», *Journal of Neural Engineering*, set. 2020, doi: 10.1088/1741-2552/abb581.

[3] Y. Tachibana, H. Iwamuro, H. Kita, M. Takada, e A. Nambu, «Subthalamo-pallidal interactions underlying parkinsonian neuronal oscillations in the primate basal ganglia», *European Journal of Neuroscience*, vol. 34, n. 9, pagg. 1470–1484, nov. 2011, doi: 10.1111/j.1460-9568.2011.07865.x.

[4] A. Sharott, F. Vinciati, K. C. Nakamura, e P. J. Magill, «A Population of Indirect Pathway Striatal Projection Neurons Is Selectively Entrained to Parkinsonian Beta Oscillations», *The Journal of Neuroscience*, vol. 37, n. 41, pagg. 9977–9998, ott. 2017, doi: 10.1523/JNEUROSCI.0658-17.2017.

[5] R. Levy, W. D. Hutchison, A. M. Lozano, e J. O. Dostrovsky, «Synchronized neuronal discharge in the basal ganglia of parkinsonian patients is limited to oscillatory activity», *The Journal of Neuroscience: The Official Journal of the Society for Neuroscience*, vol. 22, n. 7, pagg. 2855–2861, 2002, doi: 20026193.

[6] A. Raz, E. Vaadia, e H. Bergman, «Firing Patterns and Correlations of Spontaneous Discharge of Pallidal Neurons in the Normal and the Tremulous 1-Methyl-4-Phenyl-1,2,3,6-Tetrahydropyridine Vervet Model of Parkinsonism», *Journal of Neuroscience*, vol. 20, n. 22, pagg. 8559–8571, 2000, doi: 10.1523/JNEUROSCI.20-22-08559.2000.

[7] W.-J. Neumann *et al.*, «Subthalamic synchronized oscillatory activity correlates with motor impairment in patients with Parkinson's disease», *Movement Disorders*, vol. 31, n. 11, pagg. 1748–1751, nov. 2016, doi: 10.1002/mds.26759.

[8] A. Kumar, S. Cardanobile, S. Rotter, e A. Aertsen, «The Role of Inhibition in Generating and Controlling Parkinson?s Disease Oscillations in the Basal Ganglia», *Frontiers in Systems Neuroscience*, vol. 5, n. OCTOBER 2011, pag. 86, ott. 2011, doi: 10.3389/fnsys.2011.00086.

[9] J. Bahuguna, A. Sahasranamam, e A. Kumar, *Uncoupling the roles of firing rates and spike bursts in shaping the STN-GPe beta band oscillations*, vol. 16, n. 3. 2020.

[10] N. Mallet, B. Ballion, C. Le Moine, e F. Gonon, «Cortical inputs and GABA interneurons imbalance projection neurons in the striatum of parkinsonian rats», *Journal of Neuroscience*, vol. 26, n. 14, pagg. 3875–3884, apr. 2006, doi: 10.1523/JNEUROSCI.4439-05.2006.

[11] H. Cagnan *et al.*, «Temporal evolution of beta bursts in the parkinsonian cortical and basal ganglia network», *Proceedings of the National Academy of Sciences of the United States of America*, vol. 116, n. 32, pagg. 16095–16104, ago. 2019, doi: 10.1073/pnas.1819975116.

[12] I. Bar-Gad, G. Heimer, Y. Ritov, e H. Bergman, «Functional Correlations between Neighboring Neurons in the Primate Globus Pallidus Are Weak or Nonexistent», *Journal of Neuroscience*, vol. 23, n. 10, pagg. 4012–4016, 2003, doi: 10.1523/JNEUROSCI.23-10-04012.2003.

[13] M. Lindahl, J. H. Kotaleski, e J. Hellgren Kotaleski, «Untangling Basal Ganglia Network Dynamics and Function: Role of Dopamine Depletion and Inhibition Investigated in a Spiking Network Model», *eNeuro*, vol. 3, n. 6, nov. 2017, doi: 10.1523/ENEURO.0156-16.2016.

[14] D. J. Hegeman, E. S. Hong, V. M. Hernández, e C. S. Chan, «The external globus pallidus: Progress and perspectives», *European Journal of Neuroscience*, vol. 43, n. 10. Blackwell Publishing Ltd, pagg. 1239–1265, mag. 01, 2016, doi: 10.1111/ejn.13196.

[15] C. J. Wilson, «Active decorrelation in the basal ganglia», *Neuroscience*, vol. 250, pagg. 467–482, 2013, doi: 10.1016/j.neuroscience.2013.07.032.

[16] B. R. Miller, A. G. Walker, A. S. Shah, S. J. Barton, e G. V. Rebec, «Dysregulated information processing by medium spiny neurons in striatum of freely behaving mouse models of Huntington's disease», *Journal of Neurophysiology*, vol. 100, n. 4, pagg. 2205–2216, ott. 2008, doi: 10.1152/jn.90606.2008.

[17] N. Mallet, A. Pogosyan, L. F. Márton, J. P. Bolam, P. Brown, e P. J. Magill, «Parkinsonian beta oscillations in the external globus pallidus and their relationship with subthalamic nucleus activity», *Journal of Neuroscience*, vol. 28, n. 52, pagg. 14245–14258, dic. 2008, doi: 10.1523/JNEUROSCI.4199-08.2008.

[18] R. Brette e W. Gerstner, «Adaptive Exponential Integrate-and-Fire Model as an Effective Description of Neuronal Activity», *Journal of Neurophysiology*, vol. 94, n. 5, pagg. 3637–3642, nov. 2005, doi: 10.1152/jn.00686.2005.

[19] C. Linssen *et al.*, «NEST 2.16.0», 2018, doi: 10.5281/ZENODO.1400175.

[20] R. Rosenbaum, M. A. Smith, A. Kohn, J. E. Rubin, e B. Doiron, «The spatial structure of correlated neuronal variability», *Nature Neuroscience*, vol. 20, n. 1, Art. n. 1, 2017, doi: 10.1038/nn.4433.

[21] I. E. Ohiorhenuan, F. Mechler, K. P. Purpura, A. M. Schmid, Q. Hu, e J. D. Victor, «Sparse coding and high-order correlations in fine-scale cortical networks», *Nature*, vol. 466, n. 7306, Art. n. 7306, 2010, doi: 10.1038/nature09178.

[22] D. K. Leventhal, G. J. Gage, R. Schmidt, J. R. Pettibone, A. C. Case, e J. D. Berke, «Basal ganglia beta oscillations accompany cue utilization», *Neuron*, vol. 73, n. 3, pagg. 523–536, feb. 2012, doi: 10.1016/j.neuron.2011.11.032.

[23] G. Tinkhauser *et al.*, «The modulatory effect of adaptive deep brain stimulation on beta bursts in Parkinson's disease», *Brain*, vol. 140, n. 4, pagg. 1053–1067, apr. 2017, doi: 10.1093/brain/awx010.

[24] A. Pavlides, S. J. Hogan, e R. Bogacz, «Computational Models Describing Possible Mechanisms for Generation of Excessive Beta Oscillations in Parkinson's Disease», *PLOS Computational Biology*, vol. 11, n. 12, pag. e1004609, dic. 2015, doi: 10.1371/journal.pcbi.1004609.